iJRASET
International Journal For Research in Applied Science and Engineering Technology



INTERNATIONAL JOURNAL FOR RESEARCH

IN APPLIED SCIENCE & ENGINEERING TECHNOLOGY

Volume: 14 **Issue:** V **Month of publication:** May 2026

DOI: https://doi.org/10.22214/ijraset.2026.82276

www.ijraset.com

Call: 08813907089 | E-mail ID: ijraset@gmail.com

International Journal for Research in Applied Science & Engineering Technology (IJRASET)
ISSN: 2321-9653; IC Value: 45.98; SJ Impact Factor: 7.538
Volume 14 Issue V May 2026- Available at www.ijraset.com

Design of Compact Single Element Antenna for Wideband Communication Systems

Goutam Mahto
Department of Electronics and Communication Engineering RTC Institute of Technology Ranchi, India

Abstract: ***The design and analysis of a small wideband single antenna that operates in the 2.6 GHz to 8 GHz frequency range for contemporary wireless communication applications are presented in this work. The suggested antenna is built on a FR-4 substrate with compact dimensions and a dielectric constant of 4.3. Throughout the operational band, the antenna has good radiation characteristics and a broad impedance bandwidth. Within the targeted frequency range, the simulated results demonstrate acceptable return loss, VSWR, gain, and radiation efficiency. WLAN, WiMAX, C-band, and other broadband communication systems are among the wireless applications that the antenna supports. The suggested antenna is appropriate for wideband wireless devices since its radiation pattern is consistent across working frequencies. The suggested antenna is a good option for contemporary communication applications due to its small size, straightforward design, and broad working bandwidth.***

Index Terms: Wideband antenna, Single antenna, FR-4 substrate, WLAN, WiMAX, C-band, Wireless communication.

I. INTRODUCTION

Compact, wideband antennas that can operate across several frequency bands are in high demand due to the quick expansion of contemporary wireless communication systems [1]–[3]. WLAN, WiMAX, satellite communication, radar systems, C-band communication, and broadband wireless networks are just a few of the many wireless applications that require wideband antennas [4]–[7]. Antennas with high bandwidth, consistent radiation properties, and small size are ideal to serve these applications.Due to their low profile, light weight, low fabrication cost, and simple integration with microwave circuitry, microstrip antennas have attracted a lot of attention. However, the bandwidth of traditional microstrip antennas is typically limited [8]–[10]. As a result, creating a small antenna with increased bandwidth has grown to be a significant field of study in contemporary antenna engineering [11]–[13].A small single wideband antenna that operates between 2.6 GHz and 8 GHz is suggested and examined in this paper [14]–[17]. The FR-4 substrate used in the antenna's design has a dielectric constant of 4.3 and a thickness of 1.6 mm [18], [18]–[20]. With respectable return loss, VSWR, gain, and radiation efficiency throughout the working frequency range, the suggested antenna offers a broad impedance spectrum [21]–[23]. Additionally, the antenna's radiation performance is stable, which makes it appropriate for a range of wireless communication uses WLAN, WiMAX, LTE, and C-band applications are just a few of the significant communication bands that fall within the 2.6 GHz to 8 GHz working frequency range [24]–[26]. The suggested antenna's wide operational bandwidth and small design make it suitable for usage in contemporary broadband and portable wireless devices [27]–[29].

II. ANTENNA DESIGN

A. Single Element antenna Structure

The geometry of a single wideband microstrip antenna built on a FR-4 substrate is shown in the provided figure [29]. A microstrip feed line feeds a modified circular radiating patch that makes up the antenna.The width of the substrate is denoted by W [30]. The length of the substrate is denoted by L. The FR-4 dielectric substrate used in the construction of antennas is indicated by the light blue area [31], [32]. The radiating patch element that emits electromagnetic radiation is the yellow-shaped structure. The circular radiating patch's outside radius is indicated by the letter R [33]. The inner circular slot radius created inside the patch is represented by the symbol r. The antenna is excited by the microstrip feed line, which is the thin yellow strip attached to the patch [34]. F stands for feed line width. The partial ground plane is shown by the dark blue section at the bottom.G1 indicates how long the ground plane is [35]. G2 and G3 show the distance on both sides between the feed line and the ground plane [36]. Impedance matching and bandwidth performance are enhanced by these gaps.

©IJRASET: All Rights are Reserved

ISSN: 2321-9653; IC Value: 45.98; SJ Impact Factor: 7.538
Volume 14 Issue V May 2026- Available at www.ijraset.com

The dimension of Single antenna structure as shown in Table 1. W is equal to 35 mm shows how wide the substrate is. Maintaining consistent radiation properties and impedance bandwidth is facilitated by an appropriate substrate width. L is equal to 35 mm shows how long the substrate is. Because of its small size 35 35 mm^2, the antenna can be used in portable wireless applications. R is equal to 12 mm shows the circular radiating patch's outer radius. The antenna's bandwidth and resonance frequency are primarily controlled by this parameter. (r) = 4 mm shows the inner circular slot's radius inside the patch. The slot boosts wideband performance and current distribution.G1 is equal to 10 mm shows the length of the ground plane that is partial. Wider impedance bandwidth and improved return loss are made possible by the partial ground plane. G2 = 4 mm represents the distance on the left

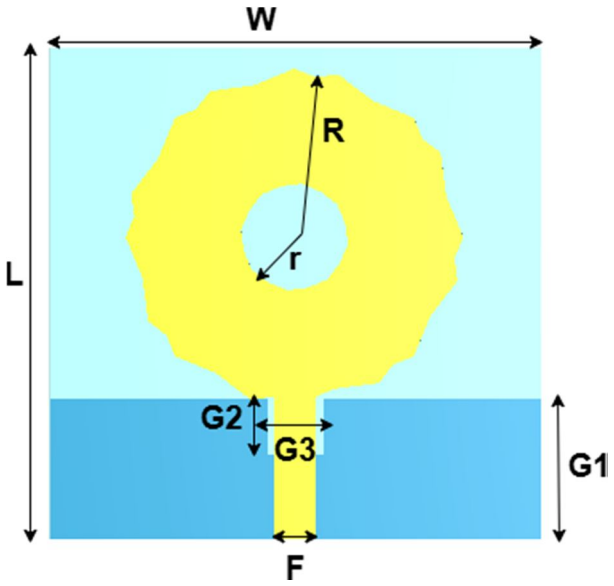


Fig. 1. Single Element antenna structure

between the ground plane and the feed line. Both impedance matching and reflection losses are reduced by this separation. G3 = 4 mm shows the distance on the right side between the ground plane and the feed line. Symmetric current flow is ensured by equal spacing on either side. F is 3 mm.indicates the microstrip feed line's width. For optimal power transfer, this width is chosen to offer a characteristic impedance of roughly 50 ohm.

TABLE I
SINGLE ELEMENT ANTENNA STRUCTURE DIMENSION

Value	Size(mm)
W	35
L	35
R	12
r	4
G1	10
G2	4
G3	4
F	3

B. Zntenna Design Evolution

The antenna design evolution as shown in figure 2. (A) Basic Rectangular Patch Antenna Structure (A) shows the original antenna design, which consists of a straightforward rectangular radiating patch coupled to a partial ground plane and microstrip feed line. This simple construction functions at a confined frequency range and has a limited bandwidth. Around the boundaries of the rectangular area, the current distribution is mostly concentrated. (B) Antenna with Circular Slot Modification The rectangular patch is changed into a circular radiating element with an inner circular slot in structure (B). Additional resonances are introduced and the surface current flow is altered by the circular slot.

©IJRASET: All Rights are Reserved

Both the operational bandwidth and impedance matching are improved by this change. The antenna starts to outperform the basic design in terms of wideband properties. (C) Final Optimized Antenna Structure Structure (C) displays the final optimized antenna geometry with further edge adjustments surrounding the circular patch. The current distribution is improved and return loss is decreased by these edge perturbations. Over the frequency range of 2.6 GHz to 8 GHz, the optimized structure offers superior bandwidth, consistent radiation characteristics, better VSWR, and higher efficiency. For contemporary wireless communication applications, the final antenna achieves a small size and wideband functioning.

In the first step, a rectangular microstrip antenna is designed, which is shown in figure 2A, whose design is by equation (1)-(4).

$$L = \frac{c}{2f_r\sqrt{\epsilon_{reff}}} - 2\Delta L \qquad (1)$$

$$\Delta L = 0.412h\frac{(\epsilon_{reff} + 0.3)(\frac{W}{h} + 0.264)}{(\epsilon_{reff} - 0.258)(\frac{W}{h} + 0.8)} \qquad (2)$$

$$\epsilon_{reff} = \frac{\epsilon_r + 1}{2} + \frac{\epsilon_r - 1}{2}\left[1 + 12\frac{h}{W}\right]^{-1/2} \qquad (3)$$

$$W = \frac{c}{2f_r\sqrt{\frac{\epsilon_r+1}{2}}} \qquad (4)$$

III. ANTENNA DESIGN SIMULATION PERFORMANCE

A. S-Parameters

The S-parameters of antenna (A), (B) and (C) as shown in figure 3. X-axis: GHz frequency, with a range of 1 to 9 GHz. Y-axis: Return Loss (S11), or S-parameter, expressed in dB.The limit of impedance matching allowable is represented by the red dashed horizontal line at –10 dB. In case S11 When the result is less than –10 dB, the antenna is deemed to function well at that frequency.

Antenna (A): the first rectangular patch antenna is shown by the black curve. The majority of the curve stays above –10 dB, indicating poor impedance matching. The antenna's resonant behavior is restricted, and its operating bandwidth is small. For wideband applications, Antenna (A) is therefore inappropriate.

Antenna (B): The redesigned antenna structure is represented by the red dotted curve. Further resonances are produced following the introduction of the circular slot. The slope falls below –10 dB at about 6 GHz, where the return loss improves. Although bandwidth performance improves over Antenna (A), it is still not entirely tuned.

Antenna (C): The final optimized antenna design is shown by the blue dashed curve. The antenna displays deep resonances in the vicinity of: 3.3 GHz and 7 GHz, around With a minimal return loss of almost –65 dB, the impedance matching is outstanding. The majority of the curve stays below –10 dB between roughly 2.6 GHz and 8 GHz, indicating broad

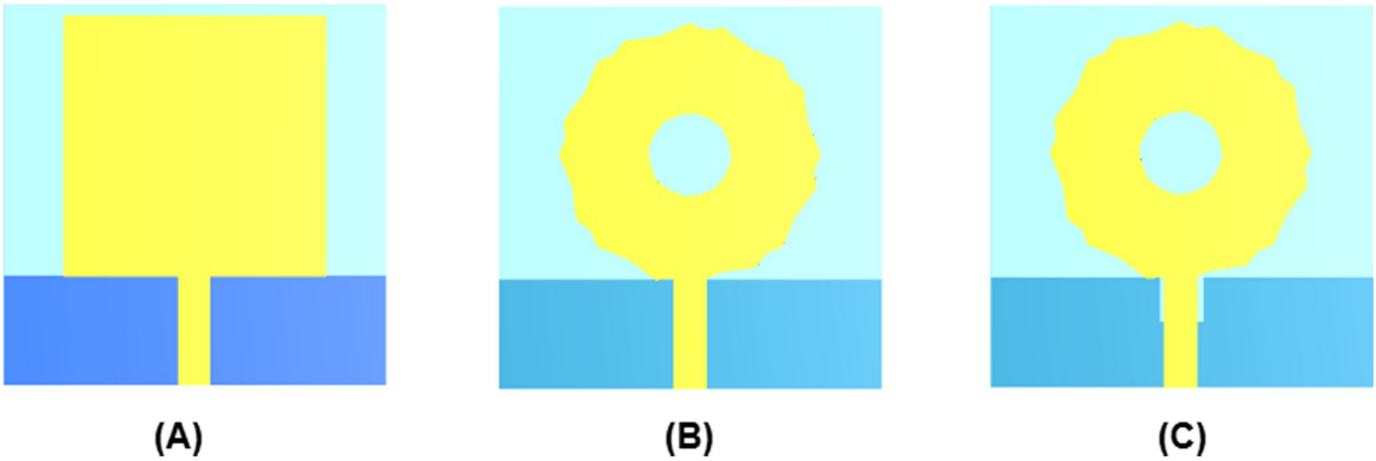


Fig. 2. Antenna design evolution: (A), (B) and (C)

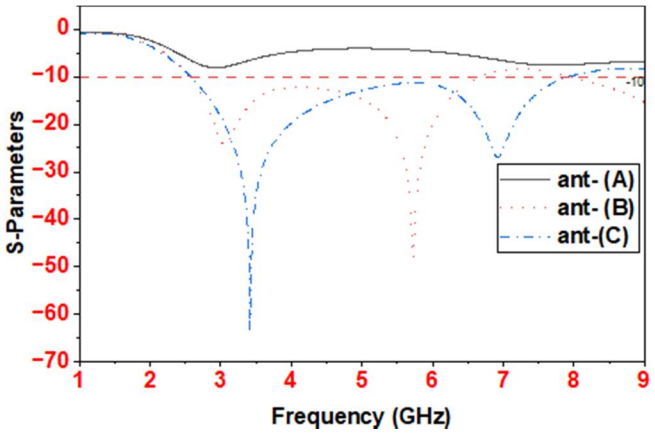


Fig. 3. S-parameters of Antenna: (A), (B) and (C)

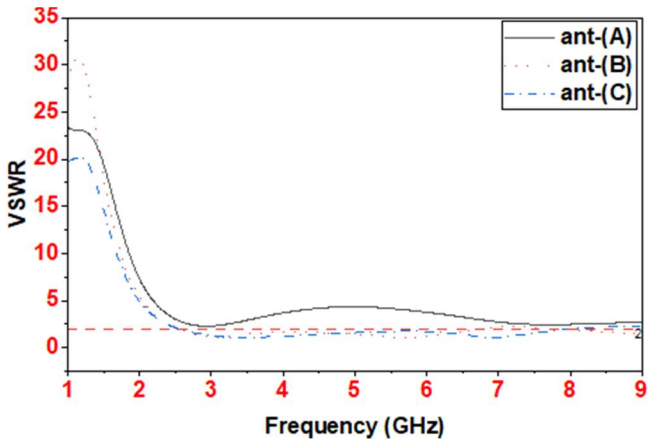


Fig. 4. VSWR of Antenna: (A), (B) and (C)

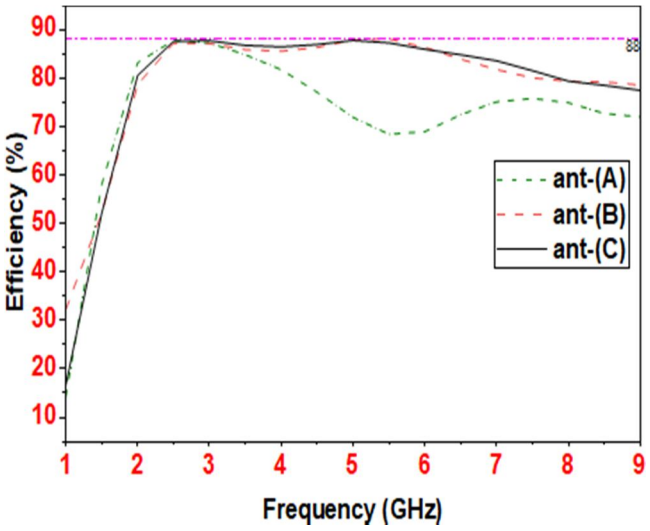


Fig. 5. % Efficiency of Antenna: (A), (B) and (C)

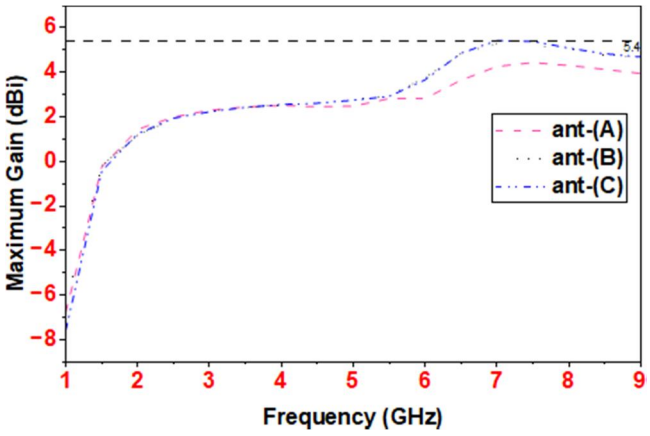


Fig. 6. Maximum gain of Antenna: (A), (B) and (C)

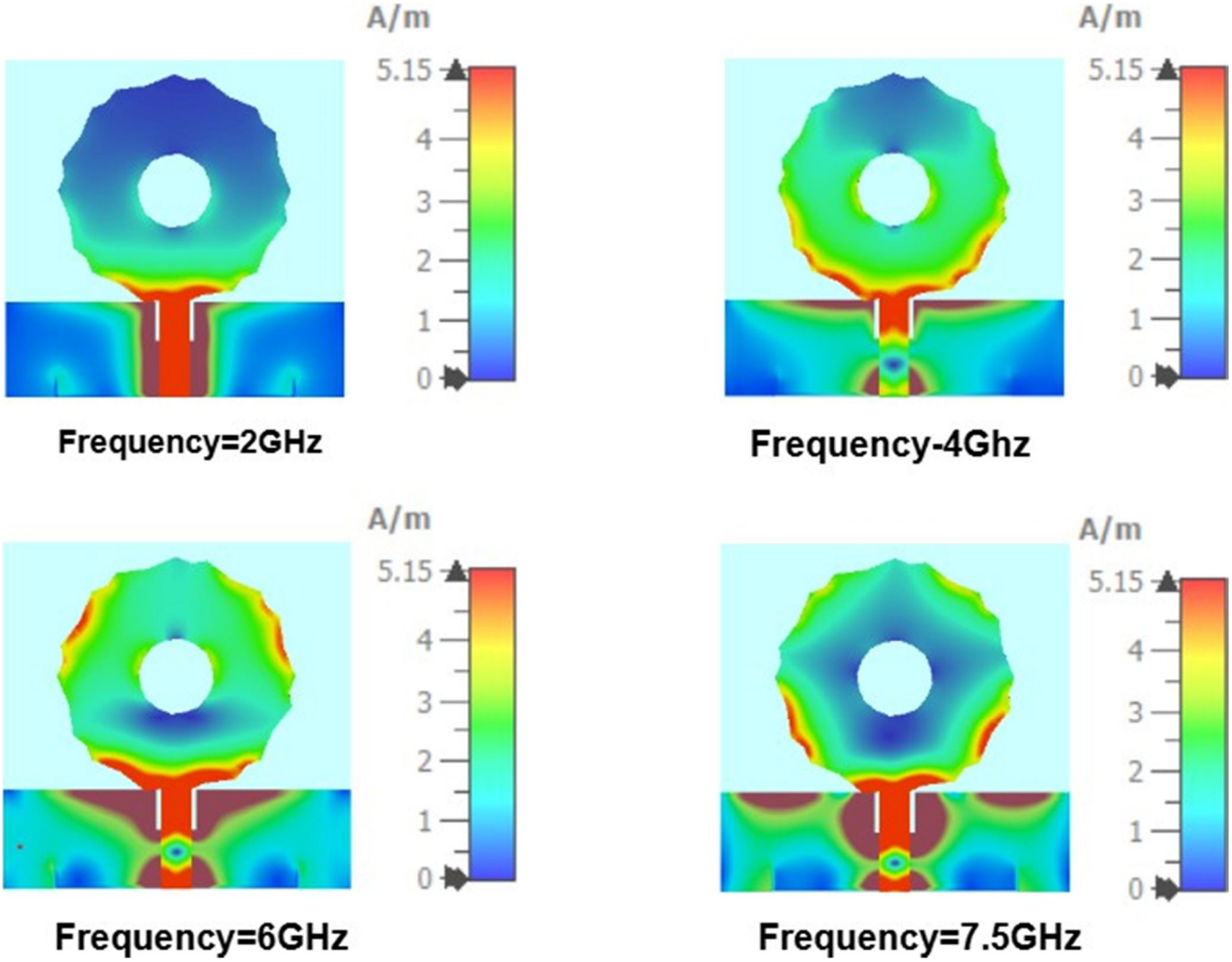


Fig. 7. Surface current distribution of antenna ant-(ant): Frequency=2Ghz,4GHz,6GHz 7.5 GHz functioning.Antenna (B) The redesigned antenna structure is represented by the red dotted curve. Further resonances are produced following the introduction of the circular slot. The slope falls below –10 dB at about 6 GHz, where the return loss improves. Although bandwidth performance improves over Antenna (A), it is still not entirely tuned.For wideband wireless communication applications operating between 2.6 GHz and 8 GHz, antenna (C) is therefore the optimal arrangement.

B. VSWR

The VSWR (Voltage Standing Wave Ratio) performance of the antenna development stages denoted as Antenna (A), Antenna (B), and Antenna (C) is shown in the graph in Figure 4. The graph illustrates how changing the antenna structure improved impedance matching.

X-axis: Frequency in GHz between 1 and 9 GHz. VSWR (Voltage Standing Wave Ratio) is the Y-axis. The standard allowable limit of VSWR=2 is shown by the red dashed horizontal line. Good impedance matching and effective powertransmission between the feed line and antenna are indicated by a VSWR value of less than 2.

Antenna (A): The original rectangular patch antenna is shown by the black curve. Poor impedance matching is indicated by a very high VSWR value at lower frequencies. Near higher frequencies, the curve progressively drops and gets closer to the permissible range. Nevertheless, the an-tenna's VSWR does not remain constant across the operational spectrum.

Antenna (B): The altered antenna construction is shown by the red dotted curve. Impedance matching is improved with the addition of the circular slot. In comparison to Antenna (A), the VSWR dramatically drops. In the operational region, most of the curve stays near or below 2.

Antenna (C): The final optimized antenna design is represented by the blue dashed curve. Out of the three structures, the antenna has the best VSWR performance. Over a large frequency range, roughly from 2.6 GHz to 8 GHz, the VSWR stays below 2. This shows minimal reflected power and superior impedance matching.Therefore, Antenna (C) is the most suitable structure for wideband wireless communication applications operating in the 2.6 GHz to 8 GHz frequency range.

C. Efficiency

The radiation efficiency (%) of the antenna evolution stages designated as Antenna (A), Antenna (B), and Antenna (C) is shown in Fig. 5. Throughout the frequency range of 1 GHz to 9 GHz, the graph shows how well the antenna transforms input power into radiated electromagnetic energy.

Antenna (A): The basic antenna structure is shown by the green dashed curve. The efficiency rises quickly from lower frequencies and approaches 2.5 GHz at about 85But above 4 GHz, the efficiency starts to decline. The efficiency drastically decreases to around 68% at 6 GHz, suggesting increased losses and erratic performance.

Antenna (B): The improved antenna structure is represented by the pink dashed curve. Over the whole operating band, the efficiency stays rather constant. Over the majority of frequencies, the antenna's efficiency remains between 85% and 88%. This improvement results from improved impedance matching and current distribution following structural alteration.

Antenna (C): The final optimized antenna design is shown by the black solid curve. High efficiency is attained by the antenna across a broad frequency range. The efficiency stays between 80% and 88% between 2.6 GHz and 8 GHz. Stable efficiency is a sign of lower dielectric and conductor losses.Consequently, for wideband wireless communication applications operating between 2.6 GHz and 8 GHz, Antenna (C) is the best design.

D. Maximum Gain

The highest gain performance of the antenna evolution stages designated Antenna (A), Antenna (B), and Antenna (C) is shown in Fig. 6. The graph illustrates how the antenna gain varies with frequency and how it increases following antenna modification.

Antenna (A): The original antenna structure is seen by the pink dashed curve. The antenna displays negative gain values at lower frequencies as a result of impedance mismatch and low radiation efficiency. The gain progressively rises with frequency. The gain approaches 4 dBi to 4.5 dBi at higher frequencies.

Antenna (B): The improved antenna structure is represented by the gray dotted curve. Following structural alteration, the gain greatly increases. Over the higher operating frequencies, the antenna attains gain values that are nearly 5 dBi. Better gain performance is a result of improved current distribution and increased bandwidth.

Antenna (C): The final optimized antenna design is shown by the blue dashed curve. Out of all the buildings, the antenna offers the most gain. The gain rises consistently with frequency, peaking between 7 and 9 GHz at 5 dBi to 5.5 dBi. The directional properties and radiation efficiency are enhanced by the improved geometry.Consequently, the optimal design for wideband wireless communication applications operating between 2.6 GHz and 8 GHz is Antenna (C).

E. Surface Current Distribution

The surface current distribution of the suggested wideband antenna at various operating frequencies—2 GHz, 4 GHz, 6 GHz, and 7.5 GHz—is depicted in Figure 7. The graphic shows the active radiating regions that are in charge of antenna operation at various frequencies and aids in the analysis of the current flow over the antenna surface.

©IJRASET: All Rights are Reserved | SJ Impact Factor 7.538 | ISRA Journal Impact Factor 7.894 |

At frequency=2GHz:The microstrip feed line and lower part of the patch are where the surface current is primarily focused at 2 GHz. Over the upper circular patch, the distribution of current is relatively poor. This suggests that the feed region and lower radiating edge are the primary sources of lower-frequency resonance.
At frequency=4GHz:The current disperses across the circular patch and slot region's bottom edges at 4 GHz. There is a significant concentration of current close to the feed connection. By adding more resonant current pathways, the altered circular geometry increases impedance bandwidth.
At frequency=6GHz:Around the patch's outer margins, the surface current becomes more evenly distributed at 6 GHz. Significant current concentration is also seen in the slot region. This symmetrical current flow enhances antenna efficiency and radiation stability.
At frequency=7.5GHz:Strong current concentration can be seen along the feed line, lower patch edges, and slot borders at 7.5 GHz. At higher frequencies, several resonant current pathways are produced. Stable current distribution is maintained by the antenna, enabling increased gain and wideband operation.

IV. Results and Discussion

The proposed antenna provides wide impedance bandwidth from 2.6 GHz to 8 GHz. The maximum gain is 5.8 dBi and efficiency is grater than 80%.The good VSWR is obtained between 1 to 2. Overall obtained performance is good for wide band ranges.The Simulation performance parameters of perposed antenna as shown in table II.

TABLE II
PERFORMANCE PARAMETERS OF PROPOSED ANTENNA

Parameter	Value
Frequency Range	2.6–8 GHz
Maximum gain	>5 dBi
VSWR	<2
Efficiency	>80%

V. CONCLUSION

A compact single-element antenna has been presented for wireless applications. The proposed antenna achieves wide bandwidth, high Efficiency, good maximum gain and good VSWR.Therefore, the antenna is suitable for modern wireless communication systems.

VI. ACKNOWLEDGEMENT

The authors would like to thank the Department of Electronics and Communication Engineering for providing support and laboratory facilities for this research work.

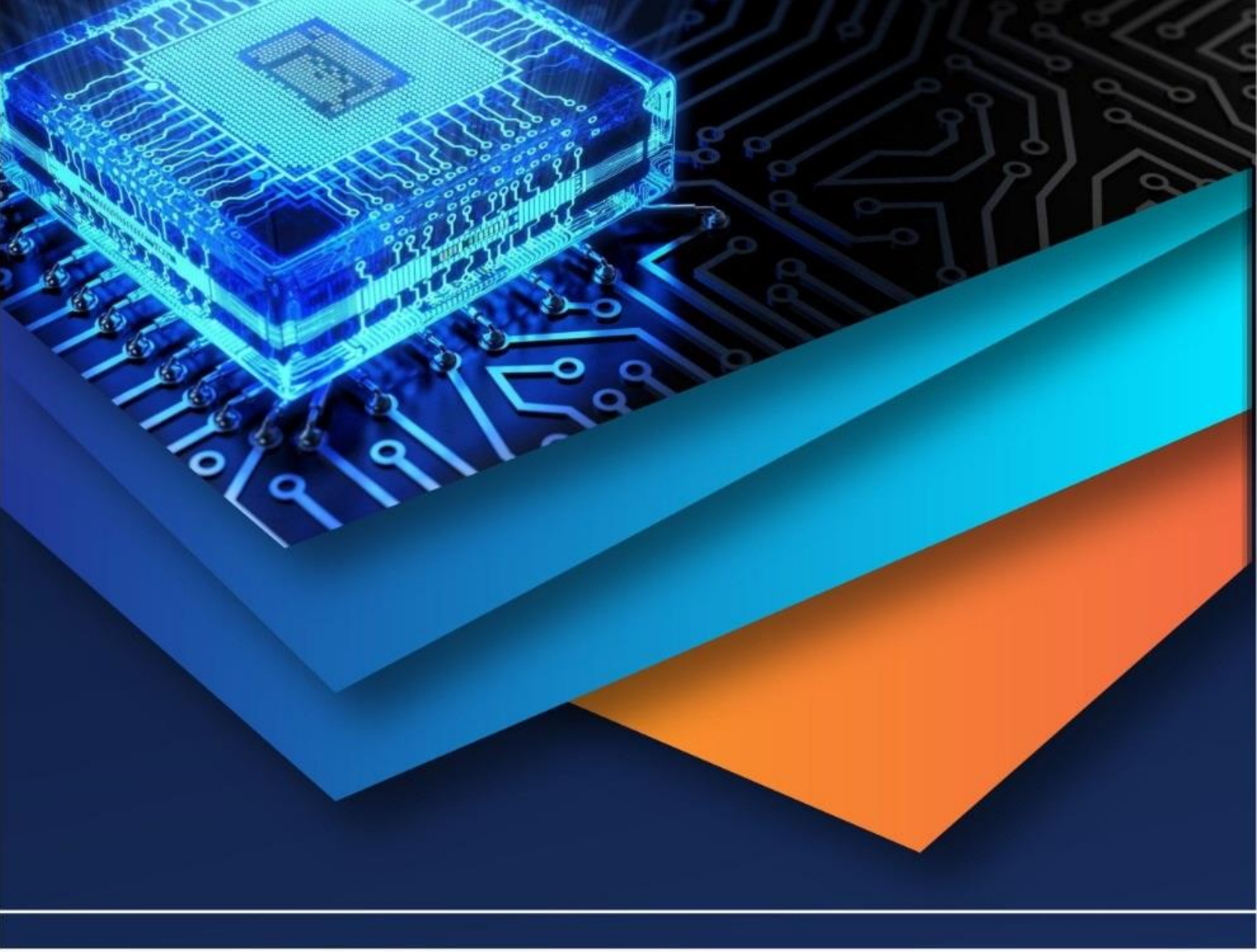
REFERENCES

[1] X.-H. Ding, Z. Tan, and S. N. Burokur, "A compact single layer dual band microstrip patch antenna for 5g terminal applications," Scientific Reports, vol. 15, no. 1, p. 8601, 2025.
[2] I. Khouyaoui, M. Elbathaoui, M. Hamdaoui, and J. Foshi, "Design, simulation, and fabrication of high-gain microstrip patch antenna arrays for 28 ghz millimeter-wave 5g applications," Physica Scripta, vol. 100, no. 4, p. 045218, 2025.
[3] X.-H. Ding, Z. Tan, and S. N. Burokur, "A compact single layer dual band microstrip patch antenna for 5g terminal applications," Scientific Reports, vol. 15, no. 1, p. 8601, 2025.
[4] R. Veeramani, J. Rameshkumar, P. Periasamy, et al., "Comparative analysis of design techniques for compact microstrip patch antenna to enhance bandwidth for 5g applications at 28 ghz," in 2025 Third International Conference on Augmented Intelligence and Sustainable Systems (ICAISS), pp. 1005–1009, IEEE, 2025.
[5] O. Aremu, O. Ajao, O. Makinde, and J. Adeniji, "Design, simulation, and performance evaluation of 2.4 ghz microstrip patch antenna arrays with power divider for uav and drone applications," International Journal of Trend in Scientific Research and Development, vol. 9, no. 2, pp. 716–724, 2025.
[6] C. Chen, "Mutual coupling reduction in a single-layer wideband triangular micorstrip patch antenna array," IEEE Antennas and Wireless Propagation Letters, 2025.
[7] A. Kamalesh, C. Ramnarayanan, J. Vijoy, and E. Sivakumar, "Microstrip patch antenna arrays for 5g and next-generation applications," in 2025 1st International Conference on Radio Frequency Communication and Networks (RFCoN), pp. 1–7, IEEE, 2025.
[8] C. F. Ding, Y. Zeng, Z.-Y. Zhang, and M. Yu, "A via-free single-layer filtering patch antenna using etched slots and stubs," IEEE Antennas and Wireless Propagation Letters, vol. 25, no. 1, pp. 399–402, 2025.

©IJRASET: All Rights are Reserved | SJ Impact Factor 7.538 | ISRA Journal Impact Factor 7.894 |

[9] M. S. Lakshmi, G. Tangirala, D. Chaitanya, S. Garikipati, T. Kumari, and S. Alluri, "Compact multi frequency reconfigurable patch antenna with single ground-plane pin diode for electronic surveillance and wireless communications," in 2025 6th International Conference on Intelligent Communication Technologies and Virtual Mobile Networks (ICICV), pp. 1581–1588, IEEE, 2025.
[10] K. K. Zaw, E. E. Khin, T. Oo, H. M. Tun, and D. Pradhan, "Compact design of 1x2 mimo microstrip patch antenna with corners trimmed for vehicle-to-vehicle communication," Journal of Novel Engineering Science and Technology, vol. 4, no. 01, pp. 12–16, 2025.
[11] C. Chen, "A single-layer single-patch dual-polarized high-gain cross-shaped microstrip patch antenna," IEEE Antennas and Wireless Propagation Letters, vol. 22, no. 10, pp. 2417–2421, 2023.
[12] W. Nie, H.-Z. Wen, K.-D. Xu, Y.-Q. Luo, X.-L. Yang, and M. Zhou, "A compact 4× 4 filtering microstrip patch antenna array with dolph-chebyshev power distribution," IEEE Open Journal of Antennas and Propagation, vol. 3, pp. 1057–1062, 2022.
[13] A. Youssef, I. Halkhams, R. El Alami, M. O. Jamil, and H. Qjidaa, "Study and design of a microstrip patch antenna array for 2.4 ghz applications," in International Conference on Digital Technologies and Applications, pp. 309–317, Springer, 2023.
[14] N.-W. Liu, Y.-D. Liang, L. Zhu, G. Fu, Y. Liu, and Y. Yun, "Electric-field null bending of a single dual-port patch antenna for colinear polarization decoupling using characteristic modes analysis," IEEE Transactions on Antennas and Propagation, vol. 70, no. 12, pp. 12247–12252, 2022.
[15] R. B. V. S. Pranav, S. M. Vijayakumar, et al., "Improved microstrip patch antenna design for high gain and low noise," in 2023 IEEE Asia Pacific Conference on Wireless and Mobile (APWiMob), pp. 107–112, IEEE, 2023.
[16] S. K. Bairappaka, A. Ghosh, J. Kumar, and A. Bhattacharya, "A compact triple band circular polarized slotted microstrip patch antenna with low frequency ratio," International Journal of RF and Microwave Computer-Aided Engineering, vol. 32, no. 12, p. e23410, 2022.
[17] G. Zalki and M. Bakhar, "Design and implementation of microstrip patch antenna arrays for 2.4 ghz applications," 2022.
[18] M. Sharma, A. K. Gupta, T. Arora, D. Pandey, and S. Vats, "Comprehen-sive analysis of multiband microstrip patch antennas used in iot-based networks," in 2023 10th International Conference on Computing for Sustainable Global Development (INDIACom), pp. 1424–1429, IEEE, 2023.
[19] Y. Gao, J. Wang, X. Wang, and Z. Sun, "Extremely low-profile dual-band antenna based on single-layer square microstrip patch for 5g mobile application," IEEE Antennas and Wireless Propagation Letters, vol. 22, no. 7, pp. 1761–1765, 2023.
[20] G. Muntoni, G. A. Casula, M. Traversari, and G. Montisci, "A wideband single-feed circularly polarized stacked patch antenna," IEEE Access, vol. 12, pp. 103380–103387, 2024.
[21] A. M. Lafta, A. R. T. Zaboun, S. Kosimova, A. Shather, H. A. Sabah, and H. Alchilibi, "Directivity improvement of mimo array antenna using novel eight element array configuration," in 2023 3rd International Conference on Advancement in Electronics & Communication Engineering (AECE), pp. 845–848, IEEE, 2023.
[22] Z. Luo, T. Su, and K.-D. Xu, "A single-layer low-profile dual-wideband monopolar patch antenna with shorting vias and parasitic annular sec-tors," IEEE Antennas and Wireless Propagation Letters, vol. 22, no. 2,
[23] pp. 432–436, 2022.
[24] O. Aremu, O. Ajao, O. Makinde, and J. Adeniji, "Design, simulation, and performance evaluation of 2.4 ghz microstrip patch antenna arrays with power divider for uav and drone applications," International Journal of Trend in Scientific Research and Development, vol. 9, no. 2,
[25] pp. 716–724, 2025.
[26] S. Chaimool, N. Prasert, and C. Rakluea, "Low-cost fr-4 metasurface-enhanced microstrip patch antenna array for wideband 5g millimeter-wave applications," in 2024 IEEE International Workshop on Antenna Technology (iWAT), pp. 118–121, IEEE, 2024.
[27] H. Wolf, R. Striker, and B. Braaten, "On the effect of scaling an array of complementary split ring resonators (csrrs) in the ground plane of a single microstrip patch antenna," in 2022 IEEE International Symposium on Antennas and Propagation and USNC-URSI Radio Science Meeting (AP-S/URSI), pp. 1450–1451, IEEE, 2022.
[28] S. A. Khader and M. Raja, "Design and analysis of single band rectangle shape antenna for c band applications and comparing return loss with the circular shape microstrip patch antenna," in AIP Conference Proceedings, vol. 2853, p. 020142, AIP Publishing LLC, 2024.
[29] S. H. Eshan, R. R. Hasan, S. Howlader, A. Iqbal, S. Forhad, S. Aliuzza-man, K. Z. Tayef, and M. A. Rahman, "X band on-body antenna design for lung cancer detection using single-walled carbon nanotubes," in 2023 8th International Conference on Robotics and Automation Engineering (ICRAE), pp. 182–186, IEEE, 2023.
[30] J. Abraham and K. Suriyan, "Analysis of tripleband single layer proximity fed 2x2 microstrip patch array antenna," International journal of electrical and computer engineering systems, vol. 13, no. 7, pp. 493–499, 2022.
[31] M. Almalki, B. Alshammari, and S. K. Podilchak, "Dual-circularly polarized single-element patch antenna with compact multiport feeding," IEEE Antennas and Wireless Propagation Letters, vol. 23, no. 2,
[32] pp. 648–652, 2023.
[33] A. Kamalesh, C. Ramnarayanan, J. Vijoy, and E. Sivakumar, "Microstrip patch antenna arrays for 5g and next-generation applications," in 2025 1st International Conference on Radio Frequency Communication and Networks (RFCoN), pp. 1–7, IEEE, 2025.
[34] W. En-Naghma, H. Halaq, and A. El Ougli, "Design, and optimization using genetic algorithms of a dual-band microstrip antenna based on defective ground structure for wireless power transmission applications," in International Conference on Digital Technologies and Applications,
[35] pp. 96–106, Springer, 2024.
[36] S. X. Ta, K. K. Nguyen, C. Dao-Ngoc, N. Nguyen-Trong, et al., "Single-layer, dual-band, circularly polarized, proximity-fed meshed patch antenna," IEEE Access, vol. 10, pp. 94560–94567, 2022.
[37] B. Panda and K. Subhashini, "Design and implementation of circular patch antenna for wi-fi 7 and 5g applications," in 2023 IEEE Wireless Antenna and Microwave Symposium (WAMS), pp. 1–5, IEEE, 2023.
[38] B. Anantha and R. S. R. Gosula, "Compact single feed dual band microstrip patch antenna with adjustable dual circular polarization," IETE journal of research, vol. 68, no. 1, pp. 216–224, 2022.
[39] M. Dwairi, E. Dwairi, and S. Moqbel, "A mimo 28.5 ghz h-shaped microstrip patch antenna for 5g applications," in 2024 Advanced Topics on Measurement and Simulation (ATOMS), pp. 46–49, IEEE, 2024.
[40] M. Dwairi, E. Dwairi, and S. Moqbel, "A mimo 28.5 ghz h-shaped microstrip patch antenna for 5g applications," in 2024 Advanced Topics on Measurement and Simulation (ATOMS), pp. 46–49, IEEE, 2024.

©IJRASET: All Rights are Reserved | SJ Impact Factor 7.538 | ISRA Journal Impact Factor 7.894 |



10.22214/IJRASET

45.98

IMPACT FACTOR: 7.129

IMPACT FACTOR: 7.429

INTERNATIONAL JOURNAL FOR RESEARCH

IN APPLIED SCIENCE & ENGINEERING TECHNOLOGY

Call : 08813907089 (24*7 Support on Whatsapp)